

# On the phantom barrier crossing and the bounds on the speed of sound in non-minimal derivative coupling theories

Israel Quiros,<sup>1, a</sup> Tame Gonzalez,<sup>1, b</sup> Ulises Nucamendi,<sup>2, c</sup> Ricardo García-Salcedo,<sup>3, d</sup> Francisco Antonio Horta-Rangel,<sup>1, e</sup> and Joel Saavedra<sup>4, f</sup>

<sup>1</sup>*Dpto. Ingeniería Civil, División de Ingeniería, Universidad de Guanajuato, Gto., México.*

<sup>2</sup>*Instituto de Física y Matemáticas, Universidad Michoacana de San Nicolás de Hidalgo, Edificio C-3, Ciudad Universitaria, CP. 58040 Morelia, Michoacán, México.*

<sup>3</sup>*CICATA - Legaria del Instituto Politécnico Nacional, 11500, México, D.F., México.*

<sup>4</sup>*Instituto de Física, Pontificia Universidad Católica de Valparaíso, Casilla 4950, Valparaíso, Chile.*

(Dated: December 14, 2024)

In this paper we investigate the so called “phantom barrier crossing” issue in a cosmological model based in the scalar-tensor theory with non-minimal derivative coupling to the Einstein’s tensor. Special attention will be paid to the physical bounds on the squared sound speed. We find that the cosmological model based in the non-minimal derivative coupling theory – this includes the pure derivative coupling case – has serious causality problems related with superluminal propagation of the scalar perturbations. Besides, despite that the theory is free of the Ostrogradsky instability, for some values of the free parameters and/or for given initial conditions, the model is also plagued by the so called Laplacian instability. We find that, although a relationship may exist, there is not strict correlation between phantom barrier crossing and superluminal speed of sound in this theory.

PACS numbers: 04.50.Kd, 04.50.Cd, 11.10.Ef, 98.80.-k, 98.80.Jk

## I. INTRODUCTION

Scalar-tensor theories [1, 2], among which the Brans-Dicke (BD) theory [3] is the prototype, have a long and hesitating history [4]. Despite that until very recently no fundamental scalar particle was found in nature, these theories have found a variety of applications both in gravitational and in cosmological contexts. In the list of famous scalar fields (this includes the prototype BD scalar field) we encounter the Higgs particle of the standard model of particles [5], the dilaton – and other moduli fields – of the effective (low-energy) string theory [6], the inflaton that accounts for the early inflationary stage of the cosmic evolution [7, 8] and the quintessence field that embodies the so called dark energy that inflates the Universe at late times [9], among others. Starting in 2013 year things changed and it seems that the first fundamental scalar particle has been finally discovered [10]. This entails that scalars and, consequently, scalar-tensor theories have to be taken seriously as feasible scenarios for physical phenomena.

The BD theory [3], as well as the more general scalar-tensor theories [1, 2], are classical theories of the gravitational field and as such these are not intended to describe quantum gravitational phenomena. However, there are indications that including higher order terms into the gravitational action makes the given theory of gravity

more compatible with quantum (renormalizable) variants [11] whose predictions can be trusted back enough into the past. One example is the addition of four-order terms like  $R_{\mu\nu\tau\rho}R^{\mu\nu\tau\rho}$ ,  $R_{\mu\nu}R^{\mu\nu}$  and  $R^2$  into the Einstein-Hilbert action that gives a class of multimass models of gravity [12] where, in addition to the usual massless excitations of the fields, there are massive scalar and spin-2 excitations with a total of 8 degrees of freedom.<sup>1</sup> In this vein it is interesting to complement the action of standard scalar-tensor theories with higher-order terms in order to have a theory more compatible with a would be quantum version. This modification would include not only terms quadratic in the curvature invariants but, also, higher-derivative terms like:  $c_1 R \partial_\mu \phi \partial^\mu \phi$ ,  $c_2 R_{\mu\nu} \partial^\mu \phi \partial^\nu \phi$ ,  $c_3 R_{\mu\nu} \phi \nabla^\mu \nabla^\nu \phi$ ,  $c_4 \nabla_\mu R \phi \partial^\mu \phi$ ,  $c_5 R \phi \nabla^2 \phi$ ,  $c_6 \nabla^2 R \phi^2$ , where  $\nabla^2 \equiv \nabla_\mu \nabla^\mu$  and  $c_1, \dots, c_6$  are coupling constants with the dimensions of length-squared.

The problem with the indiscriminated addition of higher-derivative terms is that the resulting equations of motion contain derivatives higher than second-order and this, in turn, leads to the appearance of awful and catastrophic Ostrogradsky ghosts in the theory, that makes it strongly unstable and untenable as an adequate model of gravitational phenomena. The most general possible scalar-tensor theories that contain higher order derivatives and derivative couplings in the Lagrangian and that, at the same time, lead to second-order motion equations – so that these are free of the Ostrogradsky instability – are called as “Horndeski” theories [14–17] (see [18] for a class of theories generalizing the Horndeski ones). These

<sup>a</sup>Electronic address: iquiros@fisica.ugto.mx

<sup>b</sup>Electronic address: tamegc72@gmail.com

<sup>c</sup>Electronic address: ulises@ifm.umich.mx

<sup>d</sup>Electronic address: rigarcias@ipn.mx

<sup>e</sup>Electronic address: anthort@hotmail.com

<sup>f</sup>Electronic address: joel.saavedra@ucv.cl

<sup>1</sup> The unwanted (yet tractable) property of this theory is that the massive spin-2 mode is ghost-like [13].

theories have been applied with success to describe the cosmological evolution of our Universe in different contexts [19–22]. An interesting subset of the Horndeski theories is composed of the so called scalar-tensor theories with a non-minimal derivative (kinetic) coupling, in particular those where the kinetic coupling is to the Einstein’s tensor [23–27]:  $\propto G^{\mu\nu} \partial_\mu \phi \partial_\nu \phi$ . The latter theory is characterized by its relative mathematical simplicity when compared with other Horndeski theories and also by its ability to account for the early (transient) inflationary stage, since it is able to explain in a unique manner both a quasi-de Sitter phase and an exit from it without any fine-tuned potential [23].

The action for the typical theory with non-minimal derivative coupling of the scalar with the Einstein’s tensor:  $G_{\mu\nu} \equiv R_{\mu\nu} - g_{\mu\nu} R/2$ , is given by:

$$S = \int d^4x \frac{\sqrt{|g|}}{2} [R - (\epsilon g^{\mu\nu} - \alpha G^{\mu\nu}) \partial_\mu \phi \partial_\nu \phi - 2V(\phi)] + S_m, \quad (1)$$

where we set  $8\pi G = c = \hbar = 1$ , and the coupling constant  $\alpha$  is a real number. The parameter  $\epsilon$  can take the following values:  $\epsilon = +1$  (quintessence),  $\epsilon = -1$  (phantom cosmology), and  $\epsilon = 0$  (pure derivative coupling).<sup>2</sup> In the above equation  $S_m$  is the action of the matter degrees of freedom other than the scalar field.

Theories of the type (1) have been studied in different contexts. For instance, in [28] static, spherically symmetric solutions to the gravitational field equations derived from (1) were explored and black hole solutions with a single regular horizon were found, and their thermodynamical properties were examined. Related work regarding asymptotically locally AdS and flat black holes can be found in [29], while in [30] the authors constructed the first neutron stars based in (1). The obtained construction may – in principle – constrain in a phenomenological way the free parameters of the model. Cosmological scenarios based in theories with kinetic coupling with the Einstein’s tensor have been studied in [24] in order to examine quintessence (and phantom) models of dark energy with zero and constant self-interaction potentials. It has been shown that, in general, the universe transits from one de Sitter solution to another, depending on the coupling parameter. A variety of behaviors – including Big Bang and Big Crunch solutions, and also cosmological bounce – reveals the capabilities of the corresponding cosmological model. A dynamical systems analysis of the derivative coupling model with the exponential potential has been performed in [31]. It was found that,

for the quintessence case, the stable fixed points are the same with and without the non-minimal derivative coupling, while for the pure derivative coupling (no standard canonical kinetic term) only the de Sitter attractor exists and the dark matter solution is unstable. Cosmology based in (1) has been also investigated in [32]. The latter paper points out the existence of the Laplacian instability in the theory with kinetic coupling of the scalar field with the Einstein’s tensor in the context of reheating after inflation. Particle production after inflation in the model (1) tensor has also been studied in the reference [33] by the same authors.

A very interesting – and to our opinion, central – aspect of the theory (1) was investigated in [26]. In that reference it was found that in the cosmological model based in (1) with pure derivative coupling to the Einstein’s tensor  $\epsilon = 0$ , and with  $V = 0$ , in the absence of other matter sources ( $S_m = 0$ ), the scalar behaves as pressureless matter with vanishing sound speed, so that it could be a candidate of cold dark matter. By also considering the scalar potential ( $V \neq 0$ ), it was found that the scalar field may play the role of both dark matter and dark energy. In this case, the effective equation of state (EOS) of the scalar field  $\omega_{\text{eff}}$  can cross the phantom divide [34–37]:  $\omega_\Lambda = -1$  (this is properly the EOS parameter of the cosmological constant), but this can lead to the sound speed becoming superluminal as it crosses the divide, and so is physically forbidden. Two results we find interesting in this study: i) that the crossing of the phantom divide may be linked with superluminal sound speed, and ii) that the physical limits on the sound speed are used as a basic criterion for rejection of a given cosmological model. The fact that the physical bounds on the speed of propagation of the perturbations of the field is to be taken carefully and seriously when Horndeski-type theories are under investigation, was understood also by the authors of [38]. In that reference it was shown that, when the Dirac-Born-Infeld (DBI) galileon is considered as a local modification to gravity, such as in the Solar system, the existing stable solutions always exhibit superluminality, casting doubt on the existence of a standard Lorentz invariant UV completion of that theory.<sup>3</sup>

In view of the importance of the above issue, and given that there does not exist in the bibliography a thorough discussion on the implications for cosmology of the physical bounds on the speed of sound<sup>4</sup> in the theory (1), in the present paper we shall be concentrating in the

<sup>2</sup> In this paper we refer to ‘pure derivative coupling’ – independent of the presence or absence of the self-interacting potential – to the models based in the action principle (1) without the standard kinetic term ( $\epsilon = 0$ ), i. e., there is only kinetic coupling to the Einstein’s tensor.

<sup>3</sup> There exist alternative points of view on this issue. For instance, in [39] it is shown that galileon theories satisfy an analogue of Hawking’s chronology protection conjecture. However, there are strong arguments that contradict such kinds of non-orthodox points of view on causality (for more on this issue see Ref. [40]). In this regard we recommend the clear and pedagogical discussion on this issue given in [41].

<sup>4</sup> In [26] the subject was only partially investigated, besides only the pure derivative coupling case  $\epsilon = 0$  was considered in that reference. The issue was also stated but not investigated in [42].

“ $\omega_\Lambda = -1$ ” barrier crossing issue in the model (1) by paying special attention to the physical bounds on the speed of sound squared  $c_s^2$ . These bounds are imposed by stability and causality, two fundamental principles of classical physical theories: The squared sound speed should be non-negative  $c_s^2 \geq 0$  since otherwise the cosmological model will be classically unstable against small perturbations of the background energy density (usually called as Laplacian instability). Besides, causality arguments impose that the mentioned small perturbations of the background should propagate at most at the local speed of light  $c_s^2 \leq 1$ .

In this paper we shall go as far as we can before specifying the form of the self-interaction potential, so that our discussion be as independent as it can of the specific choice of the potential. It will be shown that, the cosmological models based in (1) develop severe causality problems related with superluminal propagation of the perturbations of the scalar field. Besides, despite that the scalar-tensor theories with non-minimal derivative coupling to the Einstein’s tensor are free of the Ostrogradsky instability, for given initial conditions and/or for some values of the free parameters, the corresponding cosmological models are plagued by the Laplacian instability.

We have organized the paper in the following way. In section II we give the main assumptions on which the present work relies and the basic expressions that will be useful in the subsequent study. In section III we discuss on the computation of the sound speed squared – the one that accounts for the speed of propagation of the perturbations of the energy density – in the present model. A quite general discussion on the phantom barrier crossing in the model (1) with positive coupling  $\alpha > 0$  will be given in section IV. In section V the basic procedures considered while performing the computations are given. In order to complement our discussion, a procedure of analysis based on the properties of the dynamical system is explained in section VI. It provides a clear illustration of the failure of causality and/or of the development of instabilities, as well as of the crossing of the phantom divide along given phase space orbits. The mentioned procedure relies on the mapping of phase space orbits into a higher dimensional space spanned by the phase space variables plus an additional dimension related with physical parameters such as the effective EOS or the squared sound speed. In sections VII and VIII we perform a detailed study of the quintessence model with non-minimal derivative coupling (we consider both  $\epsilon = 1$  and  $\epsilon = 0$ , i. e., the pure derivative coupling case) for the cases when the coupling is positive ( $\alpha > 0$ ) and when  $\alpha < 0$ , respectively. The numeric computations are performed for the exponential and the power-law potentials. A thorough discussion of the results obtained in this paper will be presented in section IX and brief conclusions will be given in section X. For completeness an elementary discussion on the so called Laplacian instability is included in the appendix section XI.

## II. BASIC EQUATIONS AND SET UP

The main hypothesis of this paper is that the physical bounds on the speed of sound (squared) are viable criteria to reject physical theories like the one being investigated here. Other assumptions considered in this paper are the following:

- For simplicity of the discussion we shall focus in the vacuum case, i. e., in (1) we set  $S_m = 0$ .
- For definiteness only expanding cosmologies ( $H \geq 0$ ) will be considered.
- We consider non-negative self-interacting potential  $V \geq 0$  (non-negative energy density).
- Only the cases with  $\epsilon = 1$  (quintessence) and  $\epsilon = 0$  (pure derivative coupling) will be of interest.

As a model for the background spacetime here we assume the Friedmann-Robertson-Walker (FRW) metric with flat spatial sections, whose line element is given by:

$$ds^2 = -dt^2 + a^2(t)\delta_{ik}dx^i dx^k. \quad (2)$$

The cosmological field equations that can be derived from the action (1) read:

$$\begin{aligned} 3H^2 &= \rho_{\text{eff}}, \quad -2\dot{H} = \rho_{\text{eff}} + p_{\text{eff}}, \\ \ddot{\phi} + 3H\dot{\phi} &= \frac{-6\alpha H\dot{H}\dot{\phi} - V'}{\epsilon + 3\alpha H^2}, \end{aligned} \quad (3)$$

where the comma denotes derivative with respect to the scalar field:  $V' \equiv dV/d\phi$ . The effective energy density and pressure of the scalar field are given by

$$\rho_{\text{eff}} = \frac{\epsilon + 9\alpha H^2}{2}\dot{\phi}^2 + V(\phi), \quad (4)$$

$$p_{\text{eff}} = \frac{\epsilon - 3\alpha H^2}{2}\dot{\phi}^2 - V(\phi) - \alpha\dot{\phi}^2\dot{H} - 2\alpha H\dot{\phi}\ddot{\phi}, \quad (5)$$

respectively. From the above equations one obtains that:

$$\begin{aligned} \rho_{\text{eff}} + p_{\text{eff}} &= (\epsilon + 9\alpha H^2)\dot{\phi}^2 - \alpha\dot{\phi}^2\dot{H} \\ &\quad - 2\alpha H\dot{\phi}\ddot{\phi}. \end{aligned} \quad (6)$$

An interesting property of the effective energy density  $\rho_{\text{eff}}$  in (4) and of the effective pressure  $p_{\text{eff}}$  in (5), is that these quantities depend not only on the scalar field matter degree of freedom  $\phi$  and its derivatives  $\dot{\phi}$  and  $\ddot{\phi}$ , but also on the curvature through  $H^2$  and  $\dot{H}$ . In the particular case of the effective kinetic energy density of the scalar field in the right-hand-side (RHS) of the Friedmann equation above:  $(\epsilon + 9\alpha H^2)\dot{\phi}^2/2$ , it is contributed not only by

$\dot{\phi}$  but also by the curvature through the squared Hubble rate.<sup>5</sup>

With the help of the first equation in (3) and of (4) one can rewrite the Friedmann equation and, correspondingly, the effective energy density, in the following way:

$$3H^2 = \gamma^2 \rho_\phi = \rho_{\text{eff}}, \quad \gamma = \frac{1}{\sqrt{1 - 3\alpha\dot{\phi}^2/2}}, \quad (7)$$

where  $\gamma = \gamma(\dot{\phi})$  is the 'boost' function and

$$\rho_\phi = \epsilon \frac{\dot{\phi}^2}{2} + V(\phi),$$

is the standard energy density of the scalar field. Written in the latter form  $\rho_{\text{eff}}$  is a function only of the scalar field degree of freedom  $\phi$ , and of its derivative  $\dot{\phi}$  since the curvature effects are hidden in the non-canonical form of the effective energy density, i. e., in the boost function.

We point out that for negative coupling ( $\alpha < 0$ ), the boost function is bounded from below and also from above:  $0 < \gamma \leq 1$ , while for positive coupling ( $\alpha > 0$ ):  $1 \leq \gamma < \infty$ , i. e., it is bounded from below only.

#### A. Non-negative coupling $\alpha$ and upper bound on $|\dot{\phi}|$

If we consider non-negative  $\alpha \geq 0$  exclusively, from (7) it follows that since  $3H^2$  should be non-negative then:  $2 - 3\alpha\dot{\phi}^2 \geq 0$ , i. e.

$$0 \leq \dot{\phi}^2 \leq \frac{2}{3\alpha} \Leftrightarrow -\frac{1}{3\alpha} \leq X \leq 0, \quad (8)$$

where  $X = \partial_\mu \phi \partial^\mu \phi / 2 = -\dot{\phi}^2 / 2$ . Notwithstanding, in spite of the commonly used variable  $X$ , in this paper we prefer to use the non-negative also bounded variable:

$$x = \frac{\dot{\phi}^2}{2} = -X, \quad 0 \leq x \leq \frac{1}{3\alpha}, \quad (9)$$

i. e. it is properly the standard kinetic energy of the scalar field.

We want to point out here the non-conventional nature of the "effective" kinetic energy of the scalar field (4) under the derivative coupling when  $\alpha > 0$ . Actually, as just seen, the standard kinetic energy  $\propto \dot{\phi}^2$  is bounded from above, a strange feature not arising in standard scalar tensor theories without self-couplings. Notwithstanding, the effective kinetic energy in (4):  $\propto (\epsilon + 9\alpha H^2)\dot{\phi}^2$ , is not bounded due the curvature effects encoded in  $H^2$ .

We recall that for the negative coupling ( $\alpha < 0$ ) the variable  $x$  is not bounded from above, i. e.,  $0 \leq x < \infty$ .

### III. SOUND SPEED SQUARED

In [43] the authors derived the evolution equations for the most general cosmological scalar, vector and tensor perturbations in a class of non-singular cosmologies derived from higher-order corrections to the low-energy bosonic string action:

$$\mathcal{L} = \frac{1}{2}f(\phi, R) - \frac{1}{2}\omega(\phi)\nabla^\mu\phi\nabla_\mu\phi - V(\phi) + \mathcal{L}_q, \quad (10)$$

where  $f(\phi, R)$  is an algebraic function of the scalar field  $\phi$  and of the curvature scalar  $R$ , while  $\omega(\phi)$  and  $V(\phi)$  are functions of the scalar field. Through  $\mathcal{L}_q$  the inclusion of higher order derivative terms is allowed:

$$\mathcal{L}_q = -\frac{\lambda}{2}\xi [c_1 R_{\text{GB}}^2 + c_2 G^{\mu\nu} \partial_\mu \phi \partial_\nu \phi + c_3 \nabla^2 \phi \partial^\mu \phi \partial_\mu \phi + c_4 (\partial^\mu \phi \partial_\mu \phi)^2], \quad (11)$$

where  $\xi = \xi(\phi)$  is a function of the scalar field,  $R_{\text{GB}}^2 \equiv R_{\mu\nu\tau\lambda}R^{\mu\nu\tau\lambda} - 4R_{\mu\nu}R^{\mu\nu} + R^2$  is the Gauss-Bonnet combination, and  $\lambda, c_1, \dots, c_4$  are constants.

Our action (1) is a particular case of (10), so that the results of [43] are easily applicable to the present model (see, for instance, [26]). The Einstein's field equations that are derived from the Lagrangian (10) read:

$$G_{\mu\nu} = T_{\mu\nu}^{\text{eff}} = T_{\mu\nu}^{(\phi)} + T_{\mu\nu}^{(q)}, \quad \nabla^2 \phi - T^{(q)} = V',$$

where the comma stands for derivative with respect to  $\phi$ ,

$$T_{\mu\nu}^{(\phi)} = \partial_\mu \phi \partial_\nu \phi - \frac{1}{2}g_{\mu\nu}(\partial^\tau \phi \partial_\tau \phi) - g_{\mu\nu}V,$$

is the standard stress-energy tensor of a scalar field, while

$$T_{\mu\nu}^{(q)} = -2\frac{\partial \mathcal{L}_q}{\partial g^{\mu\nu}} - g_{\mu\nu}\mathcal{L}_q,$$

and  $T^{(q)}$  represent the contributions derived from the next to leading order corrections given by  $\mathcal{L}_q$  in equation (11) (equation (2) of [43]). These contribute towards the effective stresses and energy. In the present cosmological model based in (1) the Lagrangian (11) can be written in the following way:

$$\mathcal{L}_q = \frac{3\alpha}{2}\dot{\phi}^2 H^2,$$

where we have set  $\xi = 1$ ,  $\lambda c_2 = -\alpha$ .

For the squared speed of sound, i. e., the speed at which the scalar perturbations propagate, it is found that [26, 43]:

$$c_s^2 = 1 + \frac{(2 + Q_b)Q_d + Q_a Q_e + \frac{2Q_a^2 Q_b}{2 + Q_b}}{(2 + Q_b)(\epsilon\dot{\phi}^2 + Q_c) + 3Q_a^2}, \quad (12)$$

<sup>5</sup> Notice that when in the above equations the non-minimal derivative coupling vanishes:  $\alpha = 0$ , we recover the standard result of general relativity with minimally coupled scalar field matter.

where

$$Q_a = -2\alpha H \dot{\phi}^2, \quad Q_b = -\alpha \dot{\phi}^2, \quad Q_c = 3\alpha H^2 \dot{\phi}^2, \\ Q_d = 2\alpha \dot{H} \dot{\phi}^2, \quad Q_e = -4\alpha \dot{\phi}(\ddot{\phi} - H\dot{\phi}).$$

Equation (12) will be our master equation for determining the (squared) speed of propagation of the perturbations of the energy density in terms of the field variables  $x = \dot{\phi}^2/2$  and  $V = V(\phi)$ . For a detailed derivation of (12) within the perturbative approach we recommend the reference [43].

#### IV. PHANTOM BARRIER CROSSING FOR THE POSITIVE COUPLING ( $\alpha > 0$ )

As mentioned in the introduction, one issue of interest when one explores cosmological models of dark energy is the possibility of crossing the so called “phantom divide” barrier  $\omega_\Lambda = -1$ . Hence, it will be useful to look for the possibility of the crossing in the theory with non-minimal derivative (kinetic) coupling to the Einstein’s tensor. Here, for simplicity of the discussion, we shall consider the case with positive coupling ( $\alpha > 0$ ) exclusively. The case with negative coupling ( $\alpha < 0$ ) will be studied in detail in section VIII.

If under the assumptions exposed in the section II, with the additional choice  $\alpha > 0$ , we combine the second and third equations in (3), we obtain:

$$-2\dot{H} = R_1 + R_2, \quad (13)$$

where

$$R_1 = \frac{2FG_+\dot{\phi}^2}{2F - \alpha\dot{\phi}^2G_-}, \quad R_2 = \frac{4\alpha\dot{\phi}HV'}{2F - \alpha\dot{\phi}^2G_-}, \quad (14)$$

and we have defined:

$$F := \epsilon + 3\alpha H^2, \quad G_\pm := \epsilon \pm 9\alpha H^2. \quad (15)$$

The effective EOS parameter of the scalar field is given by:

$$\omega_{\text{eff}} = \frac{p_{\text{eff}}}{\rho_{\text{eff}}} = -1 - \frac{2}{3} \frac{\dot{H}}{H^2} = -1 + \frac{R_1 + R_2}{3H^2}, \quad (16)$$

where  $H^2$  is given by (7) and we have taken into account (13). For standard quintessence:  $\alpha = 0$ ,  $\epsilon = 1$ , the EOS parameter in (16) can be written as

$$\omega_{\text{eff}} = -1 + \frac{\dot{\phi}^2}{3H^2}, \quad (17)$$

so that, given that  $\dot{\phi}^2/3H^2$  is always non-negative, the  $\omega_\Lambda = -1$  crossing is not possible, unless additional complications are considered such as, for instance: i) non-gravitational interaction of the dark energy and dark matter components [44], ii) multiple dark energy fields like in quintom models [45, 46] or iii) extra-dimensional effects [47]. Here we shall investigate the issue within the frame of the theory (1) where the derivatives of the scalar field are non-minimally coupled to the Einstein’s tensor.

The crossing of the phantom barrier is achieved only if  $-2\dot{H}$  may change sign during the cosmic evolution. In general  $-2\dot{H}$  is a non-negative quantity. This is specially true for the standard quintessence case. In this limit  $F = G_\pm = 1$ , so that  $-2\dot{H} = \dot{\phi}^2$ , which is always a non-negative quantity. In this case

$$\omega_{\text{eff}} = \omega_\phi \geq -1.$$

In general  $F$  and  $G_+$  in (15) are positive quantities. Besides, the denominator in (14) is always non-negative. Actually, the condition  $2F - \alpha\dot{\phi}^2G_- \geq 0$  can be written explicitly as (recall our assumptions that  $\epsilon = +1, 0$  and  $\alpha > 0$ ):

$$2\epsilon \left(1 - \frac{\alpha\dot{\phi}^2}{2}\right) + 3\alpha H^2 (2 + 3\alpha\dot{\phi}^2) \geq 0,$$

which is always met given the bounds on  $\dot{\phi}^2$  in (8). Hence, the term  $R_1$  in (14) is non-negative which means that the only term in (13) that may allow for the crossing of the phantom barrier is

$$R_2 = \frac{4\alpha\dot{\phi}HV'}{2F - \alpha\dot{\phi}^2G_-}.$$

Two clear conclusions can be done: i) the crossing is due to the derivative coupling with strength  $\alpha$ , and ii) the crossing is allowed only if  $\dot{\phi}V' = \dot{V} < 0$ , i. e., if the self-interaction potential decays with the cosmic expansion. Assuming that this is indeed the case, the competition between the positive term  $R_1$  and the negative one  $R_2$  during the course of the cosmic evolution is what makes possible the flip of sign of  $-2\dot{H} = R_1 + R_2$ , and hence the crossing of the phantom barrier. Notice that for the constant potential  $V' = 0$ , as well as for the monotonically growing potential the crossing is not possible. This is true, in particular, for the growing exponential potential:  $V \propto \exp(\lambda\phi)$  with  $\lambda > 0$  for  $\dot{\phi} > 0$  or  $\lambda < 0$  for  $\dot{\phi} < 0$ , and for the power-law  $V \propto \phi^n$  with  $n \geq 0$ . This will be clearly illustrated in the discussion in the next sections.

#### V. NUMERIC STUDY

In order to quantitatively illustrate our discussion and given that the physical quantities of interest: the effective

EOS parameter  $\omega_{\text{eff}}$  (16), the sound speed squared  $c_s^2$  (12) and the deceleration parameter:

$$q = -1 - \frac{\dot{H}}{H^2} = \frac{1 + 3\omega_{\text{eff}}}{2},$$

among others, all are functions of  $(x, V)$  (recall that  $x = \dot{\phi}^2/2$ ), it will be useful to draw these parameters as surfaces in the spaces:

$$(x, V, \text{EOS}), (x, V, \text{squared sound speed}),$$

and

$$(x, V, \text{deceleration parameter}),$$

respectively. These surfaces will clearly show where the mentioned parameters take values for every pair  $(x, V)$ .

In general the geometric properties of the mentioned surfaces depend on the slope of the self-interaction potential, i. e., on the specific functional form  $V = V(\phi)$ . For that reason, in this paper, for illustrative purposes, we shall explore two specific potentials: the frequently encountered in cosmological applications exponential potential [31, 48, 49]:  $V = V_0 \exp(\lambda\phi)$  and, also, the power-law potential  $V = V_0 \phi^{2n}$  [50]. The exponential potential

$$V = V_0 e^{\lambda\phi} \Rightarrow V' = \lambda V, \quad (18)$$

where  $V_0$  and  $\lambda$  are real constants ( $V_0 \geq 0$ ), can be found as well in higher-order or higher-dimensional gravity theories [52], and in string or Kaluza-Klein type models, where the moduli fields may have effective exponential potentials [53]. Exponential potentials can also arise due to nonperturbative effects such as gaugino condensation [54]. In the present model the exponential potential has been investigated in [31], where a dynamical systems analysis was performed. The conclusion of the authors was that the derivative coupling to the Einstein's tensor does not modify the phase space dynamics of the quintessence [49]. The power-law potential

$$V = V_0 \phi^{2n} \Rightarrow V' = 2n V_0^{1/2n} V^{1-1/2n}, \quad (19)$$

where  $V_0$  is a non-negative constant and  $n$  is a real parameter, is also frequently found in the cosmological applications [50]. In the quintessence case the inverse-power law potential exhibits the tracker behavior, a very desirable property for the quintessence if one wants to avoid the cosmic coincidence problem [51]. The origin of this potential might be associated with supersymmetry considerations [55].

The results of the numeric investigation are shown in the figures FIG. 1-FIG. 4. The figure FIG. 3 is for the positive coupling ( $\alpha > 0$ ), while FIG. 4 is for the negative coupling ( $\alpha < 0$ ). In these figures the surfaces  $\omega_{\text{eff}} = \omega_{\text{eff}}(x, V)$ ,  $c_s^2 = c_s^2(x, V)$  and  $q =$

$q(x, V)$  represent the geometrical loci where the effective EOS, the squared sound speed and the deceleration parameter, respectively, can take values for all possible pairs  $(x, V)$ . Hence, any possible trajectory in the space  $(x, V, \text{EOS})$ , in  $(x, V, \text{squared sound speed})$  or in  $(x, V, \text{deceleration parameter})$ , that can be associated with a potential cosmic history, necessarily (and entirely) lies on the mentioned surfaces. The same is true for other cosmological parameters of physical interest, such as the effective energy density, etc.

## VI. PHASE SPACE EMBEDDINGS ( $\alpha > 0$ )

Let us investigate the asymptotic properties of the dynamical system corresponding to the cosmological equations (3) in the phase plane

$$\psi = \{(x, V) : 0 \leq x \leq (3\alpha)^{-1}, V \geq 0\},$$

where for sake of simplicity and just for illustration, we are considering the positive coupling case ( $\alpha > 0$ ) exclusively. It can be demonstrated that the second order cosmological field equations (3) can be traded by the following system of 2 ordinary differential equations on the variables  $x, V$ :

$$\begin{aligned} \dot{x} &= -\frac{2x\sqrt{3(1-3\alpha x)(\epsilon x + V)}[\epsilon(1-2\alpha x) + \alpha V]}{\epsilon(1-3\alpha x + 6\alpha^2 x^2) + \alpha V(1+3\alpha x)} \\ &\quad - \frac{(1-3\alpha x)(1-\alpha x)\sqrt{2x}V'}{\epsilon(1-3\alpha x + 6\alpha^2 x^2) + \alpha V(1+3\alpha x)}, \\ \dot{V} &= \sqrt{2x}V'. \end{aligned} \quad (20)$$

Before we go any further we want to underline that here we do not care about dimensionless and bounded variables of the phase space since, what we look for, is to set a course of the cosmic history in terms of the cosmic time  $t$ , no more. A detailed dynamical systems study of the present model can be found in [31].

Different orbits  $(x(t), V(t)) \in \psi$  will correspond to possible patterns of cosmological evolution that are sustained by the dynamical system (20) and, consequently, by the cosmological equations (3). Moreover, every possible orbit that can be generated by every possible choice of the initial conditions, represents a potential cosmic history for our universe. The critical points of the dynamical system (20) correspond to “outstanding” or generic cosmological solutions of (3).

A crude inspection of (20) reveals that, independent of the specific functional form of the self-interaction potential, among the equilibrium configurations of the dynamical system in the phase plane, there is a one-dimensional critical manifold  $\mathcal{M} : (x, V) = (0, V)$  and an isolated critical point at  $x = 1/3\alpha$ , and  $V' = 0$  (i. e., for constant  $V = V_0$ , or for arbitrary potentials at  $V = 0$ , a value that, for decaying potentials, is asymptotically approached as  $\phi \rightarrow \infty$ ). Their stability properties depend

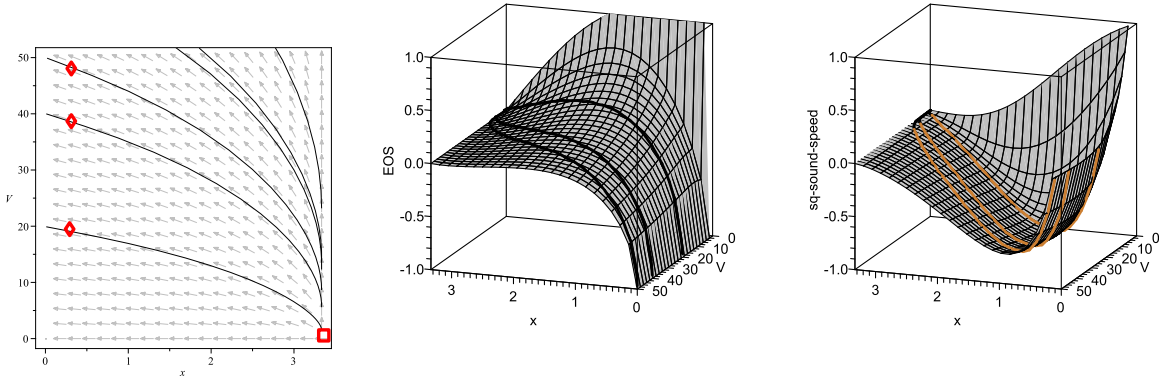


FIG. 1: Phase portrait (left) of the dynamical system (20), EOS-embedding (middle) and squared sound speed-embedding (right) diagrams for the quintessence with the kinetic coupling, for the growing exponential potential:  $V = V_0 \exp(\lambda\phi)$ , with  $\lambda = 5$ . We have chosen 6 different initial conditions (there are drawn 6 different orbits) and the coupling constant has been arbitrarily set to  $\alpha = 0.1$ . All of the orbits start at the repulsor marked with the square. Due to the unappropriated choice of the variables of the phase space, one or several equilibrium points may be lost at  $V$ -infinity. In the middle and right figures the gray surfaces represent the geometrical loci where the effective EOS parameter:  $\omega_{\text{eff}} = \omega_{\text{eff}}(x, V)$ , and the squared sound speed:  $c_s^2 = c_s^2(x, V)$ , take values for any pair  $(x, V)$ , respectively. The embedded orbits are the ones marked with the diamond in the phase portrait. The illuminated piece of the embedded orbits in the right-hand figure indicates the cosmic time interval during which the sound speed squared is negative.

on the case under study. In general every point in the manifold  $\mathcal{M}$  – but, perhaps, for the origin  $(0,0)$  – is a past attractor for given orbits (see the phase portraits in FIG. 2). For the quintessence case ( $\epsilon = 1$ ) the origin  $(0,0)$  is the future attractor, while the point  $(1/3\alpha, 0)$  is a saddle equilibrium point. Since at  $(0,0)$  the Hubble rate vanishes, i. e.,  $\rho_{\text{eff}} \rightarrow 0$ , the future attractor is the static empty universe. For the pure derivative coupling ( $\epsilon = 0$ ) the future attractor is at  $(1/3\alpha, 0)$ . At this point the effective energy density:

$$\rho_{\text{eff}} = \frac{V}{1 - 3\alpha x},$$

is undetermined. In the figure it can be appreciated that there may exist other critical points at  $V$ -infinity that are not seen in FIG. 2. In such a case an additional study of the points at infinity is required. However, as we have already mentioned, our aim here is not to perform a detailed study of the phase space asymptotics but just to establish a course of the cosmic evolution.

Now that we have established the importance of the phase space orbits for the interpretation of the cosmic history, one may wonder whether the crossing of the phantom divide, or the failure of causality, or the development of a classical instability, can be a feasible possibility in the sense that it can be sustained by the properties of the dynamical system (20). The answer is as simple as the question itself: all we have to do is to map the orbits  $(x(t), V(t)) \in \psi$  into either of the surfaces:  $\omega_{\text{eff}} = \omega_{\text{eff}}(x, V)$  or  $c_s^2 = c_s^2(x, V)$  (or  $q = q(x, V)$ , etc). The resulting procedure is what we call here as “phase space embeddings” since what we do is to embed orbits

of the phase space (one-dimensional manifolds) into surfaces (two-dimensional manifolds) associated with given physical parameters.

As a matter of fact the physical parameters  $\omega_{\text{eff}}$  and  $c_s^2$  are functions of  $x$  and  $V$  that dependent on the specific functional form of the self-interaction potential, more specifically on the slope of the potential. Hence, geometrically these parameters – let us call them generically as  $P$  – are represented by surfaces in the ‘extended’ phase space  $(x, V, P)$ . For every physically feasible choice of the variables  $x, V$ , these parameters take values on the given surfaces. The above means, in turn, that if we embed a chosen phase plane orbit into the space  $(x, V, P)$ , the resulting curve will necessarily lay on the surface  $\omega_{\text{eff}} = \omega_{\text{eff}}(x, V)$  if  $P$  is the EOS parameter, or on the surface  $c_s^2 = c_s^2(x, V)$  if  $P$  is the speed of sound squared, or on the surface  $q = q(x, V)$  if  $P$  is the deceleration parameter. One can follow the embedded orbits along the cosmic time  $t$  in order to look for crossing of the phantom divide, or for a possible failure of causality (also for the development of classical instability) during given stages of the resulting cosmic history. The results of our analysis will be then supported by the asymptotic properties of the dynamical system (20). In what follows, whereas this does not cause confusion,<sup>6</sup> the geometrical picture resulting from embedding phase space orbits into the extended phase space  $(x, V, P)$  will be called

<sup>6</sup> Do not confuse, in particular, with spacetime embedding diagram.

as “phase space embedding diagram”, or simply: “P-embedding diagram,” where  $P$  refers to the given physical parameter. Hence, the middle and right-hand figures in FIG. 1 – and also the figures in FIG. 3 and in FIG. 4 – are properly (phase space) embedding diagrams: EOS-embedding, squared sound speed-embedding and deceleration parameter-embedding diagrams, respectively.

Here for illustration we take the growing exponential potential (18) with  $\lambda > 0$  (in the calculations we have set  $\lambda = 5$ ). In FIG. 1 the phase portrait for this case is shown in the left-hand figure, while in the middle and right-hand figures the EOS and squared sound speed embedding diagrams corresponding to this case are shown. The embedded orbits in FIG. 1 are the ones marked with the diamond in the phase portrait so that one may infer where these orbits come from and where they go. As seen from the EOS-embedding diagram, there is no crossing of the phantom divide when the growing exponential potential is considered (the same is true for any other growing potentials). Besides, in this case the embedded orbits that can be associated with potential cosmic histories of the universe, transit through regions where the squared sound speed is negative – illuminated piece of the embedded orbits in the right-hand figure – signaling the occurrence of the catastrophic (classical) Laplacian instability. It can be shown that for any growing potential:  $V' > 0$ , the Laplacian instability inevitably arises. We will come back to this issue in the next sections.

## VII. PHANTOM DIVIDE CROSSING AND CONNECTION WITH SUPERLUMINALITY AND STABILITY. POSITIVE COUPLING.

In general, in terms of the variable  $x$ , the squared speed of sound is given by (12) with:

$$\begin{aligned} Q_a &= -4\alpha x H, \quad Q_b = -2\alpha x, \\ Q_c &= 6\alpha x H^2, \quad Q_d = -6\alpha x H^2 (\omega_{\text{eff}} + 1), \\ Q_e &= 8\alpha x H \left[ 4 - \frac{9\alpha H^2}{F} (\omega_{\text{eff}} + 1) + \frac{V'}{\sqrt{2xHF}} \right] \end{aligned} \quad (21)$$

where the function  $F$  is defined in (15). Meanwhile for the effective EOS (16) we have:

$$\omega_{\text{eff}} + 1 = \frac{2x(\epsilon + 3\alpha H^2)(\epsilon + 9\alpha H^2)}{3H^2\Gamma} + \frac{2\alpha\sqrt{2x}V'}{3H\Gamma}. \quad (22)$$

Hence, for the speed of sound squared (12) we get:

$$c_s^2 = 1 + \frac{4\alpha x \Pi}{(1 - \alpha x)\Gamma} - \frac{9\alpha H^2}{\Gamma}(1 - \alpha x)(\omega_{\text{eff}} + 1), \quad (23)$$

where, for compactness of writing, we have defined the following functions:

$$\begin{aligned} \Gamma &= \Gamma(x, V) \equiv \epsilon(1 - \alpha x) + 3\alpha H^2(1 + 3\alpha x), \\ \Pi &= \Pi(x, V) \equiv \epsilon(1 - \alpha x) + \alpha H^2(1 - 3\alpha x). \end{aligned} \quad (24)$$

The Hubble rate  $H$  and the boost function  $\gamma$  in the above equations, are written in terms of the variable  $x = \dot{\phi}^2/2$  as it follows:

$$\begin{aligned} 3H^2 &= \gamma^2(\epsilon x + V) \Leftrightarrow H = \gamma\sqrt{(\epsilon x + V)/3}, \\ \gamma &= \frac{1}{\sqrt{1 - 3\alpha x}}. \end{aligned} \quad (25)$$

In this section we shall consider the positive coupling case, so that the variable  $x$  is bounded from below and also from above. At the endpoints of the interval  $0 < x \leq 1/3\alpha$ , independent of  $\epsilon$  and of the type of potential – whenever  $V \neq 0$ , i. e., for non vanishing potential – the parameters  $\omega_{\text{eff}}$  and  $c_s^2$  in (22) and in (23), respectively, take the following values: At  $x = 0$ ,  $\omega_{\text{eff}} = -1$  and  $c_s^2 = 1$ , while at  $x = 1/3\alpha$  ( $H^2 \rightarrow \infty$ ),  $\omega_{\text{eff}} = 0$ ,  $c_s^2 = 0$ . In the limit when  $x \rightarrow 0$  and  $V \rightarrow 0$  simultaneously, the effective EOS parameter  $\omega_{\text{eff}}$  in (22) is undefined. In this limit:  $c_s^2 \rightarrow 1$ .

### A. Phantom barrier crossing. General analysis

Since we are considering the positive coupling case, hence:  $0 < x \leq 1/3\alpha$ . In this interval both  $\Gamma$  and  $\Pi$  in (24) are positive-valued functions. So are the factors  $\epsilon + 3\alpha H^2$ ,  $\epsilon + 9\alpha H^2$  and  $1 - \alpha x$  in (23). Recall, besides, that we are considering expanding cosmology only ( $H \geq 0$ ). The above means that the first term in the RHS of the equation for  $\omega_{\text{eff}} + 1$  in (22) is always positive. Besides, the factor  $\propto \alpha\sqrt{2x}/H$  in the second term in the RHS of this equation is also positive for all  $(x, V)$  in the  $x$ -interval considered. On the other hand the crossing of the phantom barrier is possible only if the function  $\omega_{\text{eff}} + 1$  can transit from negative to positive values and vice versa. Hence, the only possibility for the crossing in this case is that  $\omega_{\text{eff}} + 1$  can take negative values for some subset of  $\{(x, V) : 0 < x \leq 1/3\alpha, 0 \leq V\}$ . This, in turn, is possible only if the slope of the potential is negative:  $V' < 0$ , so that the second term in the RHS of the first-line equation in (23) may balance the contribution of the first term that is positive-valued for all times.

We may conclude that only decaying potentials – for instance: the decaying exponential, or the inverse power-law potentials – allow for the crossing of the phantom divide in the present model.

### B. Superluminality and Laplacian instability issues. General analysis

Given that here we concentrate in the positive coupling case ( $\alpha > 0$ ), the variable  $x$  is bounded:  $0 < x \leq 1/3\alpha$ .

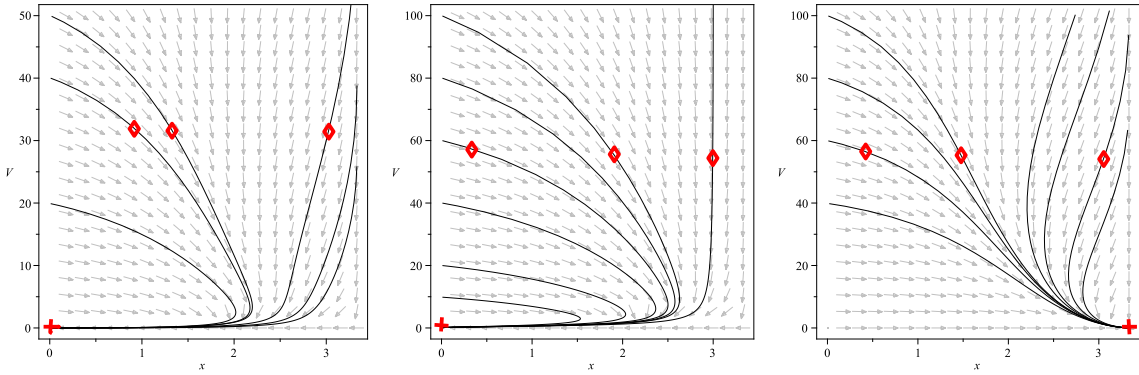


FIG. 2: From left to the right: phase portraits of the dynamical system (20) for the quintessence with kinetic coupling ( $\epsilon = 1$ ) and with the decaying exponential for  $\lambda = -5$  (left) and with the inverse power-law potential for  $n = -1$  (middle), and for the pure derivative coupling case ( $\epsilon = 0$ ) with the decaying exponential also for  $\lambda = -5$  (right), respectively.

This means, in turn that the functions  $\Gamma = \Gamma(x, V)$  and  $\Pi = \Pi(x, V)$  in (23) – the master equation for the squared sound speed  $c_s^2$  – are positive-valued real functions. Hence, the second term in the RHS of the latter equation is always positive. This entails that the mentioned term contributes towards superluminality independent of the functional form of the potential. The only way in which superluminality of the speed of sound may be avoided is for positive  $\omega_{\text{eff}} + 1 > 0$ . In this latter case the third term in the RHS of (23) may balance the contribution from the second term if:

$$4x\Pi \leq 9H^2(1 - \alpha x)^2 (\omega_{\text{eff}} + 1). \quad (26)$$

Since for monotonically decreasing potentials (potentials with negative slope) the crossing of the phantom divide  $\omega_\Lambda = -1$  is allowed, this means that in this case  $\omega_{\text{eff}} + 1$  will inevitably take negative values for some subset of  $\{(x, V) : 0 < x \leq 1/3\alpha, 0 \leq V\}$ . Hence the third term in the RHS of (23) will contribute towards superluminality as well. Once the crossing of the phantom divide is allowed, this leads to superluminality of the speed of sound being inevitable.

We want to point out that, even when the crossing of the phantom divide inevitably leads to superluminal propagation of the perturbations of the energy density, the crossing is not a necessary condition for superluminality. Actually, let us assume that  $\omega_{\text{eff}} + 1 < 0$  for all times, i. e., that  $\omega_{\text{eff}} < -1$  always, so that the crossing will never happen. In this case both the second and the third terms in the second line of (23) will boost superluminal speed of sound. Even in the case when  $\omega_{\text{eff}} + 1$  is positive for all times (no crossing), provided that the condition (26) is not fulfilled, the speed of propagation of the perturbations of the energy density in the model (1) will exceed the local speed of light.

An unwanted consequence of having positive  $\omega_{\text{eff}} + 1 > 0$ , i. e.,  $\omega_{\text{eff}} > -1$ , is that whenever the condition

$$(1 - \alpha x)\Gamma + 4\alpha x\Pi < 9\alpha H^2(1 - \alpha x)^2(\omega_{\text{eff}} + 1), \quad (27)$$

is fulfilled, the squared sound speed is negative ( $c_s^2 < 0$ ), which means in turn that a (classical) Laplacian instability inevitably develops. Hence, the present model may develop not only causality problems but, also, a Laplacian instability issue.

These issues have been explored numerically and the results are shown in the figures in FIG. 3. In the left-hand and in the middle columns panels the numerical results for the decaying exponential with  $\lambda = -5$  and for the inverse power-law potential with  $n = -1$  are displayed, respectively. We have arbitrarily chosen the coupling parameter  $\alpha = 0.1$ . In the top panels the EOS-embedding diagrams are drawn, while in the middle and in the bottom panels the squared speed of sound-embedding and the deceleration parameter-embedding diagrams are shown, respectively. It is seen that in both cases – decaying exponential and inverse power law potentials – the crossing of the phantom divide happens for given orbits, i. e., for given initial conditions. In order to make visible the crossing, the parts of the embedded orbits for which  $\omega_{\text{eff}} < -1$  have been illuminated. In a similar way, with the aim to differentiate the parts of the embedded orbits for which violations of causality occur from those where causality is satisfied, the pieces for which  $c_s^2 > 1$  have been illuminated. It is clearly shown that those embedded orbits that do the cross also violate causality. On the contrary orbits that do not cross the phantom divide meet causality (orbit without illuminated piece). The cost of this desirable behavior is that the resulting cosmic history is completely dominated by decelerated expansion (see the bottom embedding diagrams where the illuminated pieces of the trajectories indicate negative deceleration parameter, i. e. accelerated expansion). We want to underline that, as we have shown above, the crossing itself is not a necessary condition for superlumi-

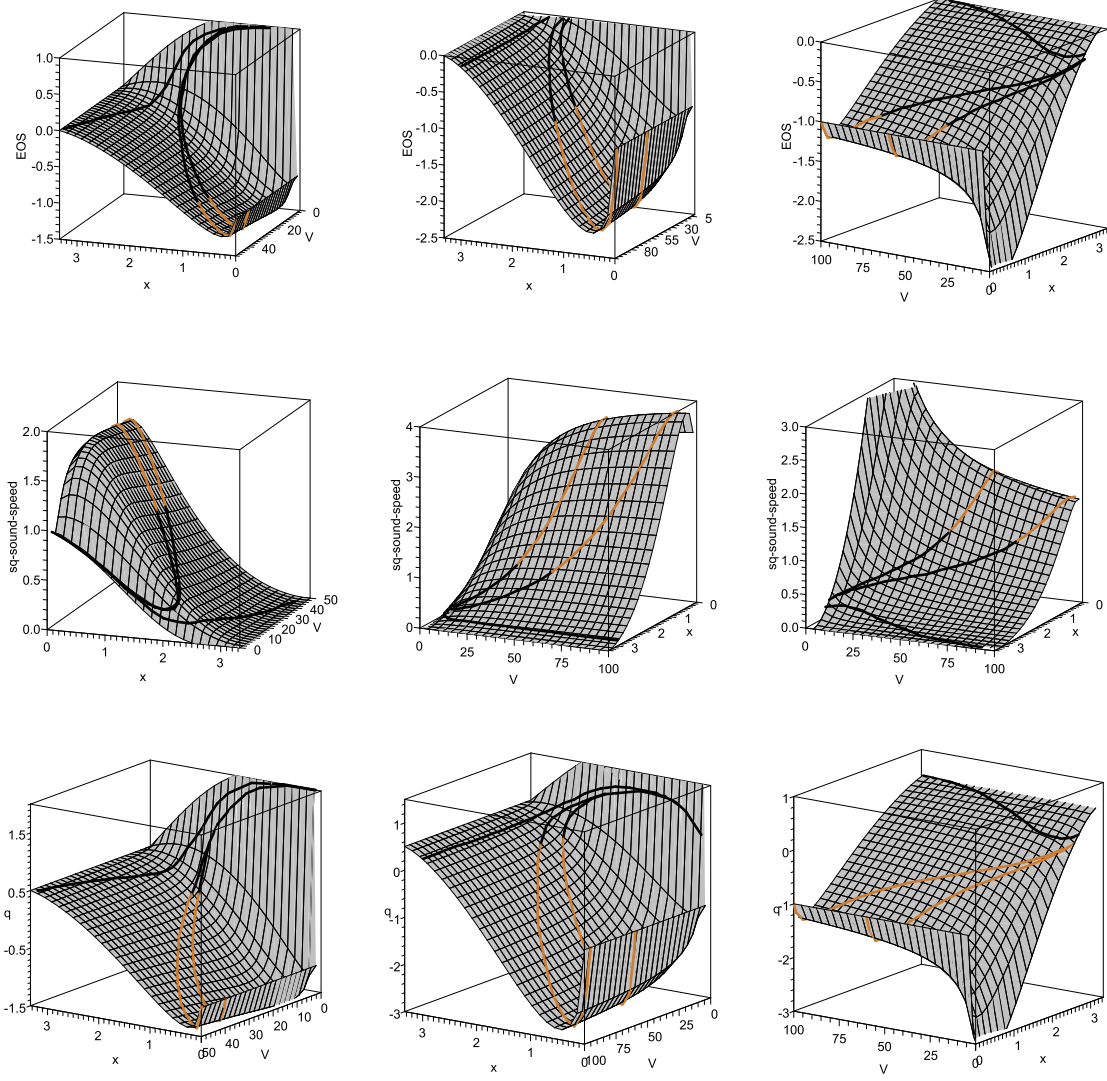


FIG. 3: EOS-embedding (top panels), squared sound speed-embedding (middle panels) and  $q$ -embedding (bottom panels) diagrams, corresponding to: a) quintessence with kinetic coupling ( $\epsilon = 1$ ) with the decaying exponential  $V = V_0 \exp(\lambda\phi)$  ( $\lambda = -5$ ) – left, b) quintessence with the kinetic coupling with the inverse power-law potential  $V = V_0 \phi^{-1}$  – middle, and c) pure derivative coupling ( $\epsilon = 0$ ) also with the decaying exponential ( $\lambda = -5$ ) – right. The embedded orbits are the ones marked with the diamond in the phase portraits in FIG. 2. In the top figures the illuminated piece of the orbits corresponds to the condition  $\omega_{\text{eff}} < -1$ . Meanwhile, in the middle row figures the illuminated portion of the embedded orbits corresponds to superluminal propagation of the scalar perturbations  $c_s^2 > 1$ , and in the bottom figures the piece of the embedded orbits that has been illuminated indicates that  $q < 0$  (accelerated expansion).

nality. The fact that in the figures in FIG. 3 the crossing of the phantom divide and superluminality seem to be tightly correlated is due to the choice of the free parameters and of the initial conditions.

### C. Pure derivative coupling ( $\epsilon = 0$ )

In this particular case the expressions for the effective EOS parameter and for the squared sound speed become

$$\omega_{\text{eff}} = -1 + \frac{6\alpha x}{1 + 3\alpha x} + \frac{2\sqrt{6x(1 - 3\alpha x)^3}}{3(1 + 3\alpha x)} \frac{V'}{\sqrt{V^3}}, \quad (28)$$

or

$$\omega_{\text{eff}} = - \left( \frac{1 - 3\alpha x}{1 + 3\alpha x} \right) \left[ 1 - \sqrt{6x(1 - 3\alpha x)} \frac{2V'}{3\sqrt{V^3}} \right], \quad (29)$$

and

$$c_s^2 = 1 + \frac{4\alpha x(1 - 3\alpha x) - 9(1 - \alpha x)^2(\omega_{\text{eff}} + 1)}{3(1 - \alpha x)(1 + 3\alpha x)}, \quad (30)$$

respectively.

From equation (29) it is seen that at the upper bound-ary:  $x = 1/3\alpha$ , the effective (background) fluid behaves like pressureless dust and, provided that the expression within square brackets in the RHS of (29) is positive:

$$1 \geq 1 - \sqrt{6x(1 - 3\alpha x)} \frac{2V'}{3\sqrt{V^3}} > 0,$$

then  $\omega_{\text{eff}} > -1$  always (for all  $t$ -s). This is specially true for potentials with positive slope (for instance, for the growing exponential and for the power-law with positive power). Hence, for the latter potentials the crossing of the phantom divide is not possible. On the contrary, for potentials with the negative slope the crossing may occur. Take, for instance, the exponential potential with  $\lambda = -\bar{\lambda}$  ( $\bar{\lambda} > 0$ ):

$$V = V_0 e^{-\bar{\lambda}\phi} \Rightarrow \frac{2V'}{3\sqrt{V^3}} = -\frac{2\bar{\lambda}}{3\sqrt{V}}.$$

Hence, provided that

$$0 \leq V < \left(\frac{2}{3}\right)^3 \left(\frac{\bar{\lambda}}{\alpha}\right)^2 \frac{(1 - 3\alpha x)^3}{2x} \Rightarrow \omega_{\text{eff}} < -1,$$

and the crossing may happen. Notice that in this case the effective EOS parameter is always a non-positive quantity ( $\omega_{\text{eff}} \leq 0$ ). A similar situation is found if choose the inverse power-law potential:  $V = V_0 \phi^{-2\bar{n}}$  ( $\bar{n} > 0$ ). In this case,

$$\frac{2V'}{3\sqrt{V^3}} = -\frac{4\bar{n}}{3V_0^{1/2\bar{n}}} V^{\frac{1-\bar{n}}{2\bar{n}}},$$

and the condition for the crossing of the phantom divide translates into the following condition on the potential:

$$V^{\frac{\bar{n}-1}{\bar{n}}} < \left(\frac{2}{3}\right)^3 \left(\frac{\bar{n}}{\alpha}\right)^2 \frac{(1 - 3\alpha x)^3}{V_0^{1/\bar{n}} x}.$$

It is seen from (30) that, whenever the crossing of the phantom divide happens, the speed of propagation of the perturbations of the background exceeds the local speed of light. Actually, for the crossing it is necessary that

$\omega_{\text{eff}} + 1 < 0$  at some stage of the cosmic evolution.<sup>7</sup> But in such a case the second term in the RHS of (30) would be positive that means, in turn, that  $c_s^2 > 1$ .

The numeric results for the decaying exponential potential (we have chosen  $\lambda = -5$  just as illustration) are shown in the right-hand panels of FIG. 3. As for the case with  $\epsilon = 1$ , depending on the chosen initial conditions, there are embedded orbits that do the crossing of the phantom divide – orbits with an illuminated piece in the right-hand panels in FIG. 3 – while others do not (orbit without illuminated piece). As seen from these figures, for the orbit that does not the crossing the expansion occurs at a decelerated pace all the time, i. e., for this orbit there is not place for the accelerated expansion of the universe to occur.

### VIII. PHANTOM DIVIDE CROSSING: CONNECTION WITH SUPERLUMINALITY AND STABILITY. NEGATIVE COUPLING.

An interesting situation arises when we consider the negative coupling case:  $\alpha = -\bar{\alpha}$  ( $\bar{\alpha} > 0$ ). As a matter of fact in many studies of the model (1) negative  $\alpha$ -s have been considered [23, 24, 26]. Here we shall be concentrating in the case when  $\epsilon = 1$ .

The first important difference when negative  $\alpha$ -s are considered is that the variable  $x = \dot{\phi}^2/2$  is not constrained to a finite interval but, in this case:  $0 \leq x < \infty$ . In the second place, notice that, given that  $\alpha = -\bar{\alpha}$  ( $\bar{\alpha} \geq 0$ ) is a negative quantity, the term  $R_2$  in (13) – see the definition in (14) – will contribute toward the change of sign of  $\dot{H}$  only if the slope of the potential is positive, in particular for the growing exponential and for the power law  $\propto \phi^{2n}$  with positive  $n$ . This is in contrast to the case with positive  $\alpha > 0$  where only potentials with negative slope will make possible the crossing of the phantom divide. In the third place, the crossing of the phantom divide may happen even for flat (constant) potentials. Take, for instance, the constant potential  $V = V_0$ . In this case we can write:

$$-2\dot{H} = \frac{(3m_0 - 2)(2\bar{\alpha}x - m_0)x}{2(1 + 3\bar{\alpha}x)[6\bar{\alpha}^2x^2 + (2 - 3m_0)\bar{\alpha}x + m_0]},$$

where for compactness of writing we have introduced the constant  $m_0 \equiv 1 - \bar{\alpha}V_0$ . Assuming the denominator of the above expression is positive, the change of sign of  $\dot{H}$  occurs at  $x = m_0/2\bar{\alpha}$ .

<sup>7</sup> We recall that the crossing itself is not a necessary condition for superluminality, instead the inequality  $\omega_{\text{eff}} + 1 < 0$  is a sufficient condition for the violations of causality to arise. Under an appropriate choice of the initial conditions one may have phase space trajectories for which the latter condition is fulfilled for all times, i. e., no crossing of the phantom divide  $\omega_{\text{eff}} + 1 = 0$  happens for these trajectories.

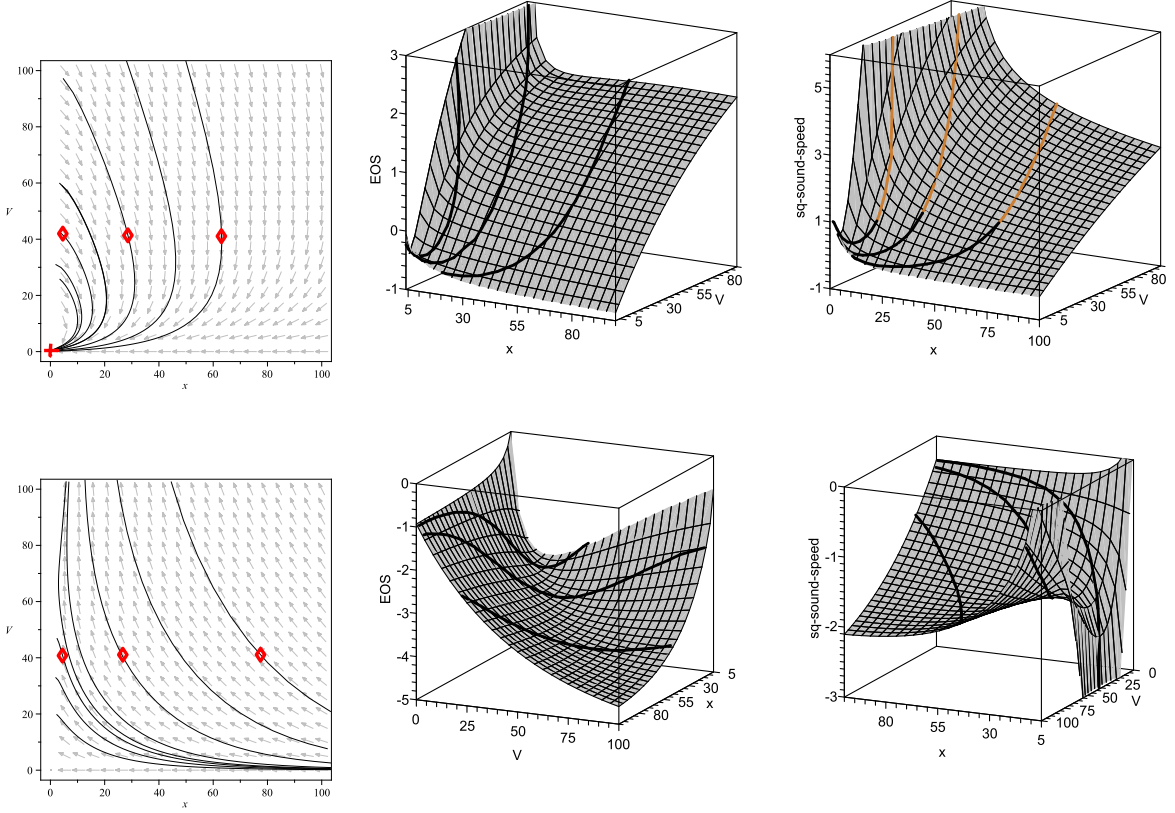


FIG. 4: Phase portrait (left) and embedding diagrams for the exponential quintessence with kinetic coupling to the curvature for negative coupling  $\alpha = -\bar{\alpha}$  (we have chosen  $\bar{\alpha} = 0.1$ ). The top panels are for the decaying exponential ( $\lambda = -1.5$ ) while the bottom panels are for the growing exponential ( $\lambda = 1.5$ ). The illuminated piece of the embedded orbits in the top right-hand figure indicates superluminal propagation of the perturbations of the background energy density ( $c_s^2 > 1$ ).

Regarding stability and causality issues, things are not better for the present model when the coupling is negative (see FIG. 4). In this case to get to general conclusions is by far a more difficult task than in the case with the positive coupling ( $\alpha > 0$ ). Our strategy in this case will be to show that there is a non-empty set of phase space trajectories – i. e. , of potential cosmic histories – that transit through stages where the squared sound speed does not meet the required physical bounds:  $0 \leq c_s^2 \leq 1$ .

Let us to rewrite the master equations for the effective EOS and for the squared sound speed for this case (recall that  $\bar{\alpha} > 0$ ):

$$\omega_{\text{eff}} + 1 = \frac{2x(1 - 3\bar{\alpha}H^2)(1 - 9\bar{\alpha}H^2)}{3H^2\bar{\Gamma}} - \frac{2\bar{\alpha}\sqrt{2x}V'}{3H\bar{\Gamma}},$$

$$c_s^2 = 1 - \frac{4\bar{\alpha}x\bar{\Pi}}{(1 + \bar{\alpha}x)\bar{\Gamma}} + \frac{9\bar{\alpha}H^2}{\bar{\Gamma}}(1 + \bar{\alpha}x)(\omega_{\text{eff}} + 1), \quad (31)$$

where we have defined:

$$\bar{\Gamma} \equiv 1 - 3\bar{\alpha}H^2 + \bar{\alpha}x(1 + 9\bar{\alpha}H^2),$$

$$\bar{\Pi} \equiv 1 - \bar{\alpha}H^2 + \bar{\alpha}x(1 - 3\bar{\alpha}H^2), \quad (32)$$

and

$$3H^2 = \frac{x + V}{1 + 3\bar{\alpha}x} = \rho_{\text{eff}}. \quad (33)$$

Notice that in the present case at the limits of the  $x$ -interval:

$$x \rightarrow 0 \Rightarrow H \rightarrow \sqrt{V/3}, \quad x \rightarrow \infty \Rightarrow H \rightarrow \sqrt{\frac{1}{3\bar{\alpha}}}.$$

Let us consider the limit  $H^2 \gg 1/\bar{\alpha}$  ( $\rho_{\text{eff}} \gg 1/\bar{\alpha}$ ). In this case we get that

$$\omega_{\text{eff}} \sim -\left(\frac{1+3\bar{\alpha}x}{1-3\bar{\alpha}x}\right) + \frac{2\sqrt{2x(1+3\bar{\alpha}x)^3} V'}{(1-3\bar{\alpha}x)\sqrt{3(x+V)^3}}, \quad (34)$$

$$c_s^2 \sim 1 - \frac{4\bar{\alpha}x(1+3\bar{\alpha}x)}{3(1-3\bar{\alpha}x)(1+\bar{\alpha}x)} + \frac{6(1+\bar{\alpha}x)}{(1-3\bar{\alpha}x)^2} \left[ 3\bar{\alpha}x - \sqrt{\frac{2x(1+3\bar{\alpha}x)^3}{3(x+V)^3}} V' \right]. \quad (35)$$

Notice from the above equations that at  $x = 1/3\bar{\alpha}$  both  $\omega_{\text{eff}}$  and  $c_s^2$  blow up. Hence  $c_s^2$  necessarily violates the physical limits on the speed of propagation of the perturbations in approaching  $x = 1/3\bar{\alpha}$ . In approaching this point from the left and from the right, depending on the potential  $V$  and on the way the phase space orbits approach to  $x = 1/3\bar{\alpha}$ , can lead to unconstrained values of different sign so that there can be violations of causality and Laplacian instability.

Suppose that the potential has negative slope:  $V' < 0$ . Hence, for those parts of the phase space trajectories at  $x < 1/3\bar{\alpha}$  the quantity  $\omega_{\text{eff}} + 1$  will be negative, i. e.  $\omega_{\text{eff}} < -1$ . In such a case  $c_s^2 > 1$  and a violation of causality arises. Actually, notice that the term in the last line of (35) is positive for  $V' < 0$  independent on the way we approach  $x = 1/3\bar{\alpha}$ : The factor  $1 - 3\bar{\alpha}x$  enters quadratically in the denominator of this term. For the same reason this term prevails over the second term in the RHS of (35) so that close enough to  $x = 1/3\bar{\alpha}$ , the squared speed of sound will be superluminal, no matter whether we approach to this point from the left ( $x \rightarrow 1/3\bar{\alpha} - 0$ ) or from the right ( $x \rightarrow 1/3\bar{\alpha} + 0$ ). The effective EOS, on the contrary, can be more negative than  $-1$  or even positive, depending on how we approach to  $x = 1/3\bar{\alpha}$ . This means that, along given orbits of the phase space the crossing of the phantom divide may happen.

In the case when the potential has positive slope, provided that

$$0 < V' < 3\bar{\alpha}\sqrt{\frac{3x(x+V)^3}{2(1+3\bar{\alpha}x)^3}}, \quad (36)$$

for the piece of the phase space trajectories at  $x < 1/3\bar{\alpha}$ , the effective EOS parameter:  $\omega_{\text{eff}} < -1$  (the opposite condition should hold at  $x > 1/3\bar{\alpha}$  in order to have  $\omega_{\text{eff}} < -1$ ). Then, given that (36) is satisfied, as  $x \rightarrow 1/3\bar{\alpha} - 0$ , the term in the last line of (35) overcomes the second one and the squared sound speed  $c_s^2 > 1$ , leading to a violation of causality. On the contrary, if approach to  $x = 1/3\bar{\alpha}$  from the right ( $x \rightarrow 1/3\bar{\alpha} + 0$ ) – assuming that the condition (36) still holds true – the squared sound speed becomes negative:  $c_s^2 < 0$  and a Laplacian instability develops.

The above explained behavior is numerically illustrated in the embedding diagrams in FIG. 4. In the top panels it is shown how for a decaying exponential potential (negative slope  $\lambda = -1.5$ ), the effective EOS

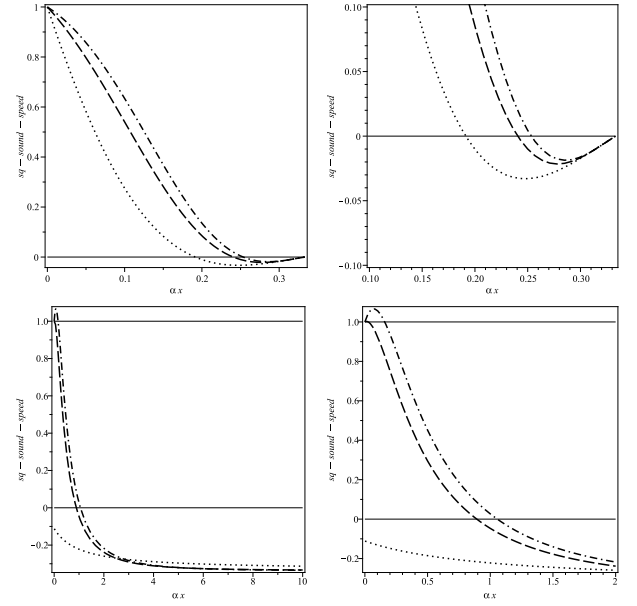


FIG. 5: Plots of the squared sound speed vs  $\alpha x$  for the constant potential  $V = V_0$ . The top figures are for the positive coupling ( $\alpha > 0$ ) while the bottom figures are for the negative coupling ( $\alpha < 0$ ). The figures in the right-hand panels show zooms of regions of interest in the corresponding left-hand panels. Three different values of the constant potential have been considered:  $V_0 = 0$  (dash-dots),  $V_0 = 0.1$  (dashed curve) and  $V_0 = 1$  (dots). Whenever these appear the thin horizontal lines represent the physical bounds on the squared sound speed:  $c_s^2 = 0$  and  $c_s^2 = 1$ , respectively.

$\omega_{\text{eff}} > -1$  for all times. This is associated with superluminal propagation of the perturbations in the right-hand figure (illuminated piece of the embedded orbits). Alternatively, for the growing exponential in the bottom panels (positive slope  $\lambda = 1.5$ ), the effective EOS is smaller than  $-1$  and the squared sound speed is always negative, signaling the occurrence of a Laplacian instability. We want to underline that in the latter case (growing potential), although the crossing of the phantom divide may in principle occur, for the chosen values of the free parameters in the numerical calculations ( $\lambda = 1.5$ ,  $\bar{\alpha} = 0.1$ ) and for the chosen embedded orbits, the crossing does not happen (see the EOS-embedding diagram in the middle figure in FIG. 4).

## IX. DISCUSSION

Our results in the previous sections are clear and convincing. These show that in general terms, without specifying the functional form of the self-interacting potential, the cosmological models based in the theory (1) – where the scalar field is kinetically coupled to the curvature – are unsatisfactory due to the inevitability of causality vi-

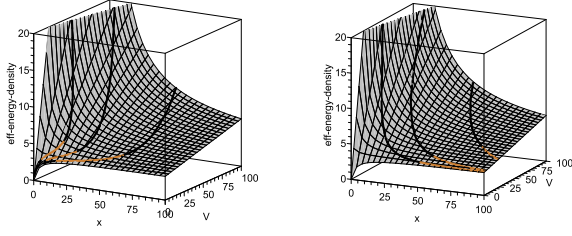


FIG. 6: Effective energy density-embedding diagram for the negative coupling  $\alpha = -0.1$ . We have chosen the decaying exponential potential ( $\lambda = -1.5$ ) – left, and the growing exponential ( $\lambda = 1.5$ ) – right, respectively. The embedded orbits are the ones marked with the diamond in the corresponding phase portraits in FIG. 4. The pieces of the embedded orbits where the effective energy density is almost a constant:  $\rho_{\text{eff}} \sim \text{const}$  (illuminated part of the orbits), can be associated with transient quasi-de Sitter phases of the cosmic evolution.

ulations and/or of the classical Laplacian instability for a non-empty set of initial conditions. We have shown this analytically for the coupling constant of either sign, and also numerically by specifying the form of the potential (we have done this for the exponential and for the power-law potentials). There is, however, a particular class of such models without the potential ( $V = 0$ ) and with the constant potential ( $V = V_0$ ) that deserve separate comments.

Before we go further, in order to unify the terminology and to be able to compare our results with other results in the bibliography, we want to make a comment on the sign of the coupling constant  $\alpha$ . This constant was named as  $\kappa$  in [23, 24],  $\alpha$  in [26],  $\zeta$  in [42] and  $\omega^2$  in [31]. If compare the action in [23] (equation (8) of that reference) – the same action as in [24] but in this case the self-interacting potential for the scalar field is considered – we see that their  $\kappa$  corresponds to  $-\alpha$  of the present paper, so that, when the authors of [23, 24] refer to negative coupling  $\kappa < 0$  this means positive coupling in terms of our  $\alpha$  ( $\alpha > 0$ ) and vice versa. We recall that in [23, 24] both cases:  $\kappa > 0$  ( $\alpha < 0$ ) and  $\kappa < 0$  ( $\alpha > 0$ ), were considered. In [26] it seems that there is a problem with the sign of the Lagrangian density in (1.5) of their work. While a straightforward comparison of the action (2.4) of [26] – with the substitution of the Lagrangian density (1.5) – with our equation (1) yields the correspondence  $\alpha \rightarrow -\alpha$  between the coupling constant in their work and in the present paper, respectively, a comparison of our cosmological field equations (3) with the corresponding equations (2.12) in [26] yields to a direct correspondence  $\alpha \rightarrow \alpha$ . Since our results are of direct importance for cosmology, here we assume that the sign of the coupling constant in [26] and in our paper coincides. In a similar way the sign of the coupling constant  $\zeta$  in [42] and  $\omega^2$

in [31] is the same as for our  $\alpha$ . The only difference is that in [31] the coupling constant  $\omega^2$  is assumed to take positive values exclusively, while in the remaining works – this includes ours – both signs are considered.

For a constant potential  $V = V_0$  – this includes the vanishing potential  $V_0 = 0$  – we have that (for definiteness we consider  $\epsilon = 1$ ):

$$3H^2 = \frac{x + V_0}{1 \mp 3\alpha x}, \quad (37)$$

where the ‘-’ sign is for the positive coupling while the ‘+’ sign is for the negative coupling (here we assume that  $\alpha$  is a positive real). Recall that for the positive coupling  $0 \leq x \leq (3\alpha)^{-1}$ , while for the negative one:  $0 \leq x < \infty$ . From (37) it follows that, for the positive coupling the Hubble rate is unbounded from above but bounded from below:  $\sqrt{V_0/3} \leq H < \infty$ . Meanwhile, for the negative coupling ( $0 \leq x < \infty$ ) the Hubble rate is bounded:

$$\frac{1}{3\sqrt{\alpha}} \leq H \leq \sqrt{\frac{V_0}{3}},$$

where we have assumed that  $V_0 > 1/3\alpha$ .

For the constant potential case the dynamical system (20) reduces to a single ordinary differential equation (ODE):

$$\dot{x} = -\frac{2x\sqrt{3(1-3\alpha)(\epsilon x + V_0)}[1 - 2\alpha x + \alpha V_0]}{1 - 3\alpha x + 6\alpha^2 x^2 + \alpha V_0(1 + 3\alpha x)}, \quad (38)$$

for the positive coupling ( $0 \leq x < 1/3\alpha$ ), or to

$$\dot{x} = -\frac{2x\sqrt{3(1+3\alpha)(\epsilon x + V_0)}[1 + 2\alpha x - \alpha V_0]}{1 + 3\alpha x + 6\alpha^2 x^2 - \alpha V_0(1 - 3\alpha x)}, \quad (39)$$

for the negative coupling ( $0 \leq x < \infty$ ). Recall that in all cases  $\alpha > 0$  and the sign of the coupling is already contained in the corresponding ODE.

The critical points of the ODE (38) are at  $x = 1/3\alpha$  and at the origin  $x = 0$ . The former is a unstable equilibrium point since linear perturbations  $\delta$  around this point ( $x \rightarrow 1/3\alpha - \delta$ ), up to an integration constant quadratically grow:

$$\delta(t) = \frac{1 + 3\alpha V_0}{12\alpha^2} t^2.$$

Alternatively, the origin is a stable equilibrium point since the linear perturbations  $\delta$  around it ( $x \rightarrow 0 + \delta$ ) exponentially decay with the cosmic time:  $\delta(t) \propto \exp(-2\sqrt{3V_0}t)$ . The above means that, for the positive coupling, the cosmic dynamics starts at  $x = 1/3\alpha$ , where  $H \rightarrow \infty$ , i. e., starts at the big bang and ends up at  $x = 0$ , where  $H = \sqrt{V_0/3}$ , i. e., ends up at a de Sitter solution. This is the standard late time behavior expected in any scalar field model with a constant potential. This

is consistent with the fact that, for the positive coupling, the late time dynamics is not modified by the kinetic coupling [23]. For the vanishing potential the asymptotic late time dynamics corresponds to the empty static universe.

Coincidentally, one of the critical points of the ODE (39): the stable point, is found at the origin ( $x = 0$ ) as well. The other critical point is at  $x \rightarrow \infty$  and due to the unappropriated choice of the phase variable, which is unbounded from above in this case ( $0 \leq x < \infty$ ), its stability properties can not be studied unless one chooses another (bounded) variable. As a matter of fact, it results that the point at  $x \rightarrow \infty$  is unstable. Hence, for the negative coupling the asymptotic dynamics starts at  $x \rightarrow \infty$  and ends up at  $x = 0$ . This means that for the negative coupling the cosmic dynamics starts at the de Sitter solution  $H = 1/3\sqrt{\alpha}$  and the end point is also a de Sitter phase with  $H = \sqrt{V_0/3}$  (for the vanishing potential the end point is the empty static universe). The asymptotic de Sitter state  $H = 1/3\sqrt{\alpha}$  is associated with the primordial inflation [23] and the fact that it is an unstable equilibrium state warrants the natural (required) exit from the early times inflationary stage. Transient quasi-de Sitter phases of the cosmic evolution can be found also for other potentials than the constant one. In the figure FIG. 6 this statement is illustrated for the decaying exponential (left) and for the growing exponential (right) potentials, respectively.

The bad news for this simple cosmological model resides in the potential violations of the physical bounds of the squared sound speed that, as shown in the former sections, are inherent in the cosmological models based in the action (1). A look at the figures in FIG. 5 confirms the latter statement: No matter whether the coupling is positive or negative, the asymptotic dynamics at early times develops a (classical) Laplacian instability that makes impossible the formation of cosmic structure. This makes very improbable that the early times (primordial) inflationary stage can be described by the cosmological model based in (1) with the constant potential (this includes the vanishing potential case).

The same problems with the violations of the physical bounds:  $0 \leq c_s^2 \leq 1$ , arise if consider arbitrary potentials (other than the constant one). In the right-hand figures in FIG. 4 – properly the squared sound speed-embedding diagrams for the negative coupling  $\alpha = -0.1$ , for the decaying ( $\lambda = -1.5$ - top) and for the growing ( $\lambda = 1.5$ -bottom) exponential potentials, respectively – it is seen that there can be violations of causality (top right-hand figure) and development of a Laplacian instability (bottom right-hand figure). For the positive coupling case with arbitrary potentials the results can only confirm our previous statements as it can be seen in section VII. As seen from the figures in FIG. 3 – see also the corresponding phase portraits in FIG. 2 to look for the course of the cosmic evolution along phase space orbits – the asymptotic early times dynamics (that which is associated with the formation of cosmic structure) is compromised by ob-

vious violations of causality for a non-empty set of initial conditions. A general demonstration of this result in section VII relies on the condition  $H \gg 1/\sqrt{\alpha}$  that can be linked with the asymptotic dynamics at early times.

Now a few comments on the pure derivative coupling case with the negative coupling  $\alpha = -\bar{\alpha} < 0$  (the case with the positive coupling was investigated in section VII). For simplicity we consider here the constant potential:  $V = V_0$ . It can be shown that in this case the master equations for the effective EOS and for the squared sound speed, respectively, can be written as it follows:

$$\omega_{\text{eff}} = - \left( \frac{1 + 3\bar{\alpha}x}{1 - 3\bar{\alpha}x} \right), \quad (40)$$

$$c_s^2 = 1 - \frac{4\bar{\alpha}x(1 + 3\bar{\alpha}x)}{3(1 + \bar{\alpha}x)(1 - 3\bar{\alpha}x)} + \frac{18\bar{\alpha}x(1 + \bar{\alpha}x)}{(1 - 3\bar{\alpha}x)^2} \quad (41)$$

We see that none of the above equations depends on the specific value  $V_0$ . Notice, also, that depending on  $x$  ( $x < 1/3\bar{\alpha}$  or  $x > 1/3\bar{\alpha}$ ) – recall that we are considering the negative coupling case so that  $x$  is unbounded:  $0 \leq x < \infty$  – the effective EOS parameter  $\omega_{\text{eff}}$  can take values more or less negative than  $-1$ . However the crossing may not happen since at  $x = 1/3\bar{\alpha}$  both  $\omega_{\text{eff}}$  and  $c_s^2$  develop vertical asymptotes and, although other physical parameters such as  $\rho_{\text{eff}}$  (as well as curvature quantities like  $H^2$ ) are finite at  $x = 1/3\bar{\alpha}$ , the ODE:

$$\dot{x} = -2\sqrt{3V_0} \frac{x\sqrt{1 + 3\bar{\alpha}x}}{1 - 3\bar{\alpha}x},$$

is also undefined at the mentioned value of  $x$ . In particular, the tangent to a given phase space orbit  $\dot{x}$  in the latter equation blows up (becomes vertical) at  $x = 1/3\bar{\alpha}$ . This means that the orbits of the phase space may not cross from  $\omega_{\text{eff}} < -1$  to  $\omega_{\text{eff}} > -1$  or vice versa. From (41) it is seen also that, in approaching  $x = 1/3\bar{\alpha}$  from both sides: from the left and from the right, severe violations of causality arise. Actually, as  $x \rightarrow 1/3\bar{\alpha} - 0$ , the third term in the RHS of (41) prevails over the second one (the one with the negative sign) and adds to 1. For  $x \rightarrow 1/3\bar{\alpha} + 0$  the second term becomes negative and, together with the third one, contribute towards  $c_s^2 > 1$ . Besides, it can be shown that at  $x \gg 1/\bar{\alpha}$ ,  $c_s^2 \approx 4.33$ , so that violations of causality are the rule and not the exception for the present case.

## X. CONCLUSION

In this paper we have investigated several problems: i) phantom barrier crossing, ii) causality and iii) classical Laplacian instability, and their potential interconnection in the model (1) where the scalar field has non-minimal derivative (kinetic) coupling to the Einstein's tensor. As far as we know this is the first time when the present model is checked in all detail against the physical bounds on the squared sound speed. We have also developed an

illustrative procedure that allows to show geometrically the evolution of given physical parameters (the effective EOS, the squared sound speed, the effective energy density, etc.) along given phase space orbits. The resulting procedure – called here as “embedding diagram” – clearly illustrates the way these parameters of physical interest evolve along potential cosmic histories. The power of the procedure relies, precisely, on the fact that each phase space orbit entails a potential cosmic history that is sustained by the dynamical system corresponding to the cosmological field equations of the model.

It has been shown that, in the positive coupling case ( $0 \leq x \leq 1/3\alpha$ ), a sufficient (but not necessary) condition for superluminality to happen is that  $\omega_{\text{eff}} < -1 \Rightarrow \omega_{\text{eff}} + 1 < 0$ , since in this case the third term in the RHS of (23):

$$c_s^2 = 1 + \frac{4\alpha x \Pi}{(1 - \alpha x)\Gamma} - \frac{9\alpha H^2(1 - \alpha x)}{\Gamma} (\omega_{\text{eff}} + 1),$$

also adds to the unity. Recall that in the above equation, for the allowed  $x$ -interval:  $0 \leq x \leq 1/3\alpha$ , the functions  $\Gamma$  and  $\Pi$  – see the definition in (24) – both are positive, as well as  $1 - \alpha x$ . Since the crossing of the phantom barrier warrants that for some  $x$ -interval  $\omega_{\text{eff}} + 1 < 0$ , then it also warrants that superluminality will happen. However, as mentioned in section VII, it is not necessary that the crossing occurs in order to have superluminal propagation of the perturbations of the background. One example can be the situation when  $\omega_{\text{eff}} + 1 < 0$  for all times. In this case violations of causality arise while the crossing does not occur.

We have also shown, both analytically and numerically, that violations of causality and the occurrence of Laplacian instability are distinctive features of the cosmological models based in the action (1) no matter what the sign of the coupling constant is. Besides, although we lack a demonstration, we suspect that these are features of galileon models in general. In particular the cubic galileon model of [58, 59] seems to suffer from the same problems. A demonstration of the latter assumption will be the subject of forthcoming work.

## ACKNOWLEDGMENTS

The authors are grateful to SNI-CONACyT for continuous support of their research activity. The work of RG-

S was partially supported by SIP20172234, SIP20160512, COFAA-IPN, and EDI-IPN grants. IQ, TG and FAH-R thank CONACyT of México for support of this research. UN also acknowledges PRODEP and CIC-UMSNH.

## XI. APPENDIX: CLASSICAL INSTABILITY DUE TO IMAGINARY SOUND SPEED

Even if the theory (1) is free of the Ostrogradsky instability (the equations of motion are second order in the derivatives), it may contain other kinds of instability since it is based in a non-standard Lagrangian. Here we shall discuss on one such kind of instability that may arise in the theory with non-minimal derivative coupling with the Einstein’s tensor due to “imaginary” sound speed.

Let  $\rho_B$  and  $p_B$  be the energy density and barotropic pressure of the FRW cosmological background (in our case these are  $\rho_\phi$  and  $p_\phi$ ). If consider small perturbations of the background energy density:  $\rho_B(t) + \delta\rho_B(\mathbf{x}, t)$ , the conservation of energy and stresses  $\nabla^\mu T_{\mu\nu} = 0$ , leads to the wave equation [56]:

$$\left(-\frac{\partial^2}{\partial t^2} + c_s^2 \frac{\partial^2}{\partial \mathbf{x}^2}\right) \delta\rho_B = 0,$$

where  $c_s^2 = dp_B/d\rho_B$  is the speed of sound squared. For positive  $c_s^2 > 0$  the solution of the above equation is

$$\delta\rho_B = \delta\rho_{B0} \exp(-i\omega t + i\mathbf{k} \cdot \mathbf{x}),$$

while for negative  $c_s^2 < 0$  it is

$$\delta\rho_B = \delta\rho_{B0} \exp(\omega t + i\mathbf{k} \cdot \mathbf{x}),$$

where  $\omega = kc_s$ , with  $k = 2\pi/\lambda$  – the wave number of the perturbation ( $a/k$  is the physical wavelength of the perturbation). In the case when  $c_s^2 < 0$ , the energy density of the perturbations uncontrollably grows resulting in a classical instability of the cosmological model. The increment of instability is inversely proportional to the wavelength of the perturbations and the models where  $c_s^2 < 0$  are violently unstable so that these should be rejected [57].

- 
- [1] Y. Fujii, K.-I. Maeda, “The Scalar-Tensor Theory of Gravitation” (Cambridge University Press, Cambridge, 2003)
  - [2] V. Faraoni, “Cosmology in Scalar-Tensor Gravity” (Kluwer Academic Publishers, 2004)
  - [3] C. H. Brans, R. H. Dicke, Phys. Rev. **124** (1961) 925-935; C. H. Brans, Phys. Rev. **125** (1962) 2194-2201
  - [4] C. H. Brans, gr-qc/0506063; AIP Conf. Proc. **1083** (2008) 34-46
  - [5] W. N. Cottingham, D. A. Greenwood, “An Introduction to the Standard Model of Particle Physics” (Cambridge University Press, 2007)
  - [6] J. E. Lidsey, D. Wands, E. J. Copeland, Phys. Rept. **337** (2000) 343-492
  - [7] A. D. Linde, Phys. Lett. B **129** (1983) 177-181; Phys. Rev. D **49** (1994) 748-754

- [8] J. E. Lidsey, A. R. Liddle, E. W. Kolb, E. J. Copeland, T. Barreiro, M. Abney, *Rev. Mod. Phys.* **69** (1997) 373-410; D. H. Lyth, A. Riotto, *Phys. Rept.* **314** (1999) 1-146
- [9] E. J. Copeland, M. Sami, S. Tsujikawa, *Int. J. Mod. Phys. D* **15** (2006) 1753-1936
- [10] G. Aad et al. (ATLAS Collaboration), *Phys. Lett. B* **716** (2012) 1-29
- [11] K. S. Stelle, *Phys. Rev. D* **16** (1977) 953-969
- [12] K. S. Stelle, *Gen. Rel. Grav.* **9** (1978) 353-371
- [13] A. Hindawi, B. A. Ovrut, D. Waldram, *Phys. Rev. D* **53** (1996) 5583-5596; *Phys. Rev. D* **53** (1996) 5597-5608
- [14] G. W. Horndeski, *Int. J. Theor. Phys.* **10** (1974) 363-384
- [15] A. Nicolis, R. Rattazzi, E. Trincherini, *Phys. Rev. D* **79** (2009) 064036
- [16] C. Deffayet, S. Deser, G. Esposito-Farese, *Phys. Rev. D* **80** (2009) 064015; C. Deffayet, G. Esposito-Farese, A. Vikman, *Phys. Rev. D* **79** (2009) 084003
- [17] S. Tsujikawa, *Lect. Notes Phys.* **892** (2015) 97-136
- [18] C. Deffayet, D. A. Steer, *Class. Quant. Grav.* **30** (2013) 214006; J. Gleyzes, D. Langlois, F. Piazza, F. Vernizzi, *Phys. Rev. Lett.* **114** (2015) no.21, 211101; *JCAP* **1502** (2015) 018; M. Zumalacárregui, J. García-Bellido, *Phys. Rev. D* **89** (2014) 064046; D. Langlois, K. Noui, *JCAP* **1602** (2016) no.02, 034
- [19] F. P. Silva, K. Koyama, *Phys. Rev. D* **80** (2009) 121301
- [20] T. Kobayashi, H. Tashiro, D. Suzuki, *Phys. Rev. D* **81** (2010) 063513
- [21] N. Chow, J. Khoury, *Phys. Rev. D* **80** (2009) 024037
- [22] K. Y. Kim, H. W. Lee, Y. S. Myung, *Phys. Rev. D* **88** (2013) 123001; S. Bhattacharya, K. F. Dialektopoulos, T. N. Tomaras, *arXiv:1512.08856*; S. Bhattacharya, P. Mukherjee, A. S. Roy, A. Saha, *arXiv:1512.03902*
- [23] S. V. Sushkov, *Phys. Rev. D* **80** (2009) 103505
- [24] E. N. Saridakis, S. V. Sushkov, *Phys. Rev. D* **81** (2010) 083510
- [25] L. N. Granda, *JCAP* **1007** (2010) 006
- [26] C. Gao, *JCAP* **1006** (2010) 023
- [27] C. Germani, A. Kehagias, *Phys. Rev. Lett.* **105** (2010) 011302
- [28] M. Rinaldi, *Phys. Rev. D* **86** (2012) 084048
- [29] A. Anabalon, A. Cisterna, J. Oliva, *Phys. Rev. D* **89** (2014) 084050; A. Cisterna, C. Erices, *Phys. Rev. D* **89** (2014) 084038
- [30] A. Cisterna, T. Delsate, M. Rinaldi, *Phys. Rev. D* **92** (2015) 044050; A. Cisterna, T. Delsate, L. Ducobu, M. Rinaldi, *Phys. Rev. D* **93** (2016) 084046
- [31] Y. Huang, Q. Gao, Y. Gong, *Eur. Phys. J. C* **75** (2015) 143
- [32] Y. Ema, R. Jinno, K. Mukaida, K. Nakayama, *JCAP* **1510** (2015) 020
- [33] R. Jinno, K. Mukaida, K. Nakayama, *JCAP* **1401** (2014) 031; Y. Ema, R. Jinno, K. Mukaida, K. Nakayama, *Phys. Rev. D* **94** (2016) 063517
- [34] R. R. Caldwell, *Phys. Lett. B* **545** (2002) 23-29; A. Vikman, *Phys. Rev. D* **71** (2005) 023515
- [35] S. Nojiri, S. D. Odintsov, *Phys. Rev. D* **72** (2005) 023003
- [36] B. Feng, X.-L. Wang, X.-M. Zhang, *Phys. Lett. B* **607** (2005) 35-41
- [37] S. Nesseris, L. Perivolaropoulos, *JCAP* **0701** (2007) 018; L. Perivolaropoulos, *JCAP* **0510** (2005) 001; W. Hu, *Phys. Rev. D* **71** (2005) 047301; L. P. Chimento, R. Lazkoz, *Phys. Lett. B* **639** (2006) 591-595
- [38] G. L. Goon, K. Hinterbichler, M. Trodden, *Phys. Rev. D* **83** (2011) 085015
- [39] C. Burrage, C. de Rham, L. Heisenberg, A. J. Tolley, *JCAP* **1207** (2012) 004
- [40] G. Goon, K. Hinterbichler, *JHEP* **1702** (2017) 134; P. Motloch, W. Hu, A. Joyce, H. Motohashi, *Phys. Rev. D* **92** (2015) 044024
- [41] G. Ellis, R. Maartens, M. A. H. MacCallum, *Gen. Rel. Grav.* **39** (2007) 1651-1660
- [42] J. B. Dent, S. Dutta, E. N. Saridakis, and J.-Q. Xia, *JCAP* **11** (2013) 058
- [43] C. Cartier, J. Hwang, E. J. Copeland, *Phys. Rev. D* **64** (2001) 103504
- [44] L. Perivolaropoulos, *JCAP* **0510** (2005) 001; W. Zimdahl, D. Pavon, *Phys. Lett. B* **521** (2001) 133-138; T. Gonzalez, I. Quiros, *Class. Quant. Grav.* **25** (2008) 175019
- [45] Z.-K. Guo, Y.-S. Piao, X.-M. Zhang, Y.-Z. Zhang, *Phys. Lett. B* **608** (2005) 177-182; W. Zhao, *Phys. Rev. D* **73** (2006) 123509
- [46] Y.-F. Cai, E. N. Saridakis, M. R. Setare, J.-Q. Xia, *Phys. Rept.* **493** (2010) 1-60
- [47] L. P. Chimento, R. Lazkoz, R. Maartens, I. Quiros, *JCAP* **0609** (2006) 004
- [48] P. G. Ferreira, M. Joyce, *Phys. Rev. Lett.* **79** (1997) 4740-4743; *Phys. Rev. D* **58** (1998) 023503
- [49] E. J. Copeland, A. R. Liddle, D. Wands, *Phys. Rev. D* **57** (1998) 4686-4690
- [50] P. J. E. Peebles, B. Ratra, *Astrophys. J.* **325** (1988) L17; B. Ratra, P. J. E. Peebles, *Phys. Rev. D* **37** (1988) 3406
- [51] C. R. Watson, R. J. Scherrer, *Phys. Rev. D* **68** (2003) 123524; A. R. Liddle, R. J. Scherrer, *Phys. Rev. D* **59** (1999) 023509; I. Zlatev, L. Wang, P. J. Steinhardt, *Phys. Rev. Lett.* **82** (1999) 896-899; P. J. Steinhardt, L. Wang, I. Zlatev, *Phys. Rev. D* **59** (1999) 123504
- [52] B. Whitt, *Phys. Lett. B* **145** (1984) 176-178; J. D. Barrow, S. Cotsakis, *Phys. Lett. B* **214** (1988) 515-518; D. Wands, *Class. Quant. Grav.* **11** (1994) 269-280
- [53] M. B. Green, J. H. Schwarz, E. Witten, "Superstring Theory" (Cambridge University Press, 1987)
- [54] B. de Carlos, J. A. Casas, C. Muñoz, *Nucl. Phys. B* **399** (1993) 623-653
- [55] P. Binetruy, *Phys. Rev. D* **60** (1999) 063502; A. Masiero, M. Pietroni, F. Rosati, *Phys. Rev. D* **61** (2000) 023504
- [56] P. J. E. Peebles, B. Ratra, *Rev. Mod. Phys.* **75** (2003) 559-606
- [57] R. Yang, J. Qi, *Eur. Phys. J. C* **72** (2012) 2095; Y.-S. Piao, *Phys. Rev. D* **79** (2009) 067301
- [58] F. P. Silva, K. Koyama, *Phys. Rev. D* **80** (2009) 121301; N. Chow, J. Khoury, *Phys. Rev. D* **80** (2009) 024037
- [59] R. De Arcia, T. Gonzalez, G. Leon, U. Nucamendi, I. Quiros, *Class. Quant. Grav.* **33** (2016) 125036